

In vitro Colon Fermentation of Soluble Arabinoxylan Is Modified Through Milling and Extrusion

Journal Article**Author(s):**

Demuth, Teresa; Edwards, Veronica; Bircher, Lea; [Lacroix, Christophe](#) ; Nyström, Laura; Geirnaert, Annelies

Publication date:

2021-08

Permanent link:

<https://doi.org/10.3929/ethz-b-000505659>

Rights / license:

[Creative Commons Attribution 4.0 International](#)

Originally published in:

Frontiers in Nutrition 8, <https://doi.org/10.3389/fnut.2021.707763>



In vitro Colon Fermentation of Soluble Arabinoxylan Is Modified Through Milling and Extrusion

Teresa Demuth¹, Veronica Edwards^{1,2}, Lea Bircher², Christophe Lacroix², Laura Nyström^{1*†} and Annelies Geirnaert^{2†}

¹ Laboratory of Food Biochemistry, Institute of Food, Nutrition and Health, ETH Zurich, Zurich, Switzerland, ² Laboratory of Food Biotechnology, Institute of Food, Nutrition and Health, ETH Zurich, Zurich, Switzerland

OPEN ACCESS

Edited by:

Alfonso Benítez-Páez,
Principe Felipe Research Center
(CIPF), Spain

Reviewed by:

Carlos Gómez-Gallego,
University of Eastern Finland, Finland
Luc Saulnier,
Institut National de la Recherche
Agronomique (INRA), France

*Correspondence:

Laura Nyström
laura.nystroem@hest.ethz.ch

†These authors share first authorship

Specialty section:

This article was submitted to
Nutrition and Microbes,
a section of the journal
Frontiers in Nutrition

Received: 10 May 2021

Accepted: 28 July 2021

Published: 25 August 2021

Citation:

Demuth T, Edwards V, Bircher L,
Lacroix C, Nyström L and Geirnaert A
(2021) *In vitro* Colon Fermentation of
Soluble Arabinoxylan Is Modified
Through Milling and Extrusion.
Front. Nutr. 8:707763.
doi: 10.3389/fnut.2021.707763

Dietary fibers such as arabinoxylan (AX) are promising food constituents to prevent particular diet-related chronic diseases because of their prebiotic properties. Arabinoxylan fermentation by the gut microbiota depends on the structural architecture of AX, which can be modified during food processing and consequently affect its prebiotic potential, but it is little investigated. Therefore, the aim of this study was to evaluate the effects of naturally occurring and processing-induced structural alterations of the soluble AX of wheat bran and rye flour on the *in vitro* human colon fermentation. It was found that fermentation behavior is strongly linked to the AX fine structure and their processing-induced modifications. The short-chain fatty acid (SCFA) metabolism, acidification kinetics, bacterial growth, and bacterial composition revealed that wheat bran AX (WBAX) was fermented faster than rye flour AX. Increased levels of bound phenolic acids resulting from processing were identified as the inhibiting factor for AX fermentation kinetics. Bacterial genera promoted by AX varied between AX source and processing type, but also between microbiota. Extruded WBAX promoted butyrate production and growth of butyrate-producing *Faecalibacterium* in the butyrogenic microbiota while it did not enhance fermentation and inhibited the growth of *Prevotella* in the propiogenic microbiota. We anticipate that the findings of this study are a starting point for further investigation on the impact of processing-induced changes on the prebiotic potential of dietary fibers prior to human studies.

Keywords: arabinoxylan, prebiotic activities, food processing, gut microbiota, *in vitro* fermentation, SCFA

INTRODUCTION

The human gut microbiota represents a diverse ecosystem, which is populated by more than 10^{14} microorganisms harboring 100 times more genes than the human genome itself and, therefore, representing a tremendous metabolic potential (1). This dynamic population has a significant contribution to human health by acting against pathogens, shaping the intestinal epithelium, regulating the host immune system, and degrading undigested food such as dietary fibers (2). Besides other environmental factors, diet plays a key role in shaping and maintaining the microbiota composition and activity (3).

The intake of dietary fibers is elementary for a healthy diet and healthy gut microbiota. Plant-based polysaccharides are resistant to digestion in the human small intestine, but are fermented by

the microbes present in the colon (4, 5). This prebiotic activity leads to the various health benefits of dietary fibers, such as increasing the formation of short-chain fatty acids (SCFA) and causing fecal bulking. However, not all dietary fibers are prebiotics as, according to the latest definition, they need to be selectively utilized by the host microorganisms conferring a health benefit (6, 7). In addition to fruits and vegetables, cereals such as rye, barley, oat, and wheat are an important source of dietary fibers in the Western human diet.

Among the common cereal grains, arabinoxylan (AX) is the primary non-starch polysaccharide. According to literature, both water-soluble and water-insoluble AX exhibit various beneficial functions in the body such as an increase in SCFA owing to its prebiotic effect (8). Although the water-soluble AX fraction only accounts for 1–2% of the total AX in grains, many of its reported health-promoting effects can be attributed to water-soluble AX. It is mainly localized in the cell walls of starchy endosperm, aleurone, and bran tissues (9). The contents and molecular fine structure, which can be evaluated by molecular weight (M_w), sugar composition, and linkage pattern, depend on the AX source. Generally, AX consists of a linear (1–4)- β -D-linked xylopyranosyl backbone, substituted with α -L-arabinofuranosyl groups at positions O-3 and/or O-2 of the β -D-Xylp residues. In addition, phenolic acids, mainly ferulic acid, can be esterified on the C(O)-5 position of arabinose (10). Water-soluble wheat flour AX contains approximately one-third linked monosubstituted xylopyranosyl groups with two-thirds double substituted, whereas rye flour AX is significantly more singly substituted (11).

Apart from the naturally given structural alterations, food processing causes additional structural modifications of AX. The application of heat, pressure, or mechanical forces induces oxidative and hydrolytic reactions, which both modify the native chemical structure (12–15). Consequently, these structural modifications influence physicochemical properties and may further affect the prebiotic potential of AX (16, 17).

Only a fraction of the human gut bacteria is able to hydrolyse and ferment AX (18, 19). Previous work showed the proliferation of beneficial *Bifidobacterium*, *Lactobacillus*, *Prevotella* and *Bacteroides* spp. after AX fermentation. Induced growth can be explained by their ability to produce hydrolytic enzymes such as endo-1,4- β -D-xylanase, α -L-arabinofuranosidases, and β -D-xylosidases. This enzymatic digestion and the resulting metabolism of released monosaccharides lead to the production of beneficial SCFA metabolites and modulates the gut environment (20–22). Various studies have shown that the *in vitro* fermentation of AX is strongly linked to the molecular fine structure of AX (23, 24). Similarly, Tuncil et al. (17) hypothesized that subtle variations in dietary fiber structures may result in altered microbiota compositions. In particular, differences in M_w and the branching of soluble cereal AX affect SCFA production and bacterial growth during *in vitro* fermentation by human fecal microbiota (20, 25). A recent study by De Paepe et al. (26) confirmed that released linear oligosaccharides are fermented more rapidly than oligosaccharides with a more complex molecule structure, such as AX. From another perspective, De Paepe et al. (26) showed that the modification of wheat bran

physicochemical properties allows control over the extent and rate of SCFA production. Another study presented that wheat bran fermentation was not influenced by a dry heat treatment (27). These studies focused on the correlation of process-induced changes with the physicochemical properties of wheat bran and its impact on *in vitro* fermentation, whereas the processing-induced changes of single prebiotic compounds, such as AX isolates, at a molecular level remain unknown (16, 28, 29). Thus far, the detailed relationship of processing-induced structural modifications of soluble AX and its effect on the prebiotic activity has not been fully elucidated yet.

Hence, the objective of this study was to investigate the effect of grain milling and extrusion on the *in vitro* colon fermentation of soluble AX isolated from wheat bran (WB) and rye flour (RF). For this purpose, the fine structure of milled and extruded WBAX and RFAX was characterized by the high-performance size exclusion chromatography-refractive index (HPSEC-RI), viscometer (VISC), right angle scattering (RALS), light angle scattering (LALS), high performance liquid chromatography-ultraviolet detection (HPLC-UV), and high-performance anion exchange chromatography-pulsed amperometric detection (HPAEC-PAD) and correlated with its prebiotic activity. The prebiotic activity of the processed AX was evaluated by means of an *in vitro* fermentation by two different cultivated human colon microbiota. Therefore, both the SCFA kinetics and microbiota composition were analyzed using quantitative PCR (qPCR) and 16S rRNA gene amplicon sequencing.

MATERIALS AND METHODS

Materials

Amicase[®], α -amylase (*Bacillus licheniformis*; Thermamyl 300 L), L-(+)-arabinose ($\geq 99\%$), L-ascorbic acid ($\geq 99\%$), caffeic acid ($\geq 95\%$), cinnamic acid ($\geq 99\%$), 3,5-dichloro-4-hydroxybenzoic acid (97%), para-coumaric acid ($\geq 98\%$), ferulic acid ($> 99\%$), formic acid (HCOOH; $\geq 98\%$), D-(+)-glucose ($\geq 99\%$), hydrogen peroxide (H_2O_2 ; 35%), para-hydroxybenzoic acid ($> 98\%$), iron(II) sulfate heptahydrate ($FeSO_4 \cdot 7H_2O$; $\geq 99\%$), magnesium sulfate ($MgSO_4$; $\geq 99\%$), meat extract, mucin from porcine stomach, pepsin from porcine gastric mucosa (250 U/ml), potassium chloride (KCl; $\geq 99\%$), protocatechuic acid ($\geq 97\%$), sinapic acid ($\geq 98\%$), sodium bicarbonate ($NaHCO_3$; $> 99\%$), sodium hydroxide (NaOH, 50% in water), sodium nitrate ($NaNO_3$; $\geq 99.5\%$), sodium phosphate dibasic dihydrate ($Na_2HPO_4 \cdot 2H_2O$; $\geq 98\%$), D-(-)-sorbitol ($\geq 99\%$), syringic acid ($\geq 95\%$), trifluoroacetic acid (CF_3COOH ; $\geq 99\%$), and vanillic acid ($\geq 97\%$) were purchased from Sigma-Aldrich Chemie GmbH (Buchs, Switzerland). D-(+)-Galactose ($\geq 99\%$), sodium azide (NaN_3 ; $> 99\%$), and D-(+)-xylose ($\geq 99\%$) were obtained from Fluka Chemie GmbH (Buchs, Switzerland). Hydrogen chloride (HCl; 37%) and sodium hydroxide (NaOH; $\geq 98\%$) were purchased from VWR International (Radnor, PA, USA). Amyloglucosidase (*Aspergillus niger*; 200 U/ml), wheat arabinoxylan (medium viscosity; $\sim 95\%$), rye arabinoxylan (high viscosity; $\sim 95\%$), lichenase (*Bacillus subtilis*; 1,000 U/ml), and protease (*Bacillus licheniformis*; 300 U/ml) were obtained from Megazyme (Bray, Ireland). Calcium chloride dihydrate,

(CaCl₂·2H₂O; >99%), manganese chloride tetrahydrate (MnCl₂·4H₂O, >98%), sodium chloride (NaCl, >99%), and zinc sulfate heptahydrate (ZnSO₄·7 H₂O, >99%) were obtained from Fischer Scientific UK Limited (Loughborough, UK). Bile salts were obtained from Oxoid AG (Pratteln, Switzerland). Bacto Tryptone™ was obtained from Becton, Dickinson, and Company (Le pont de claix, France). Polyethylene oxide (PEO-24k; M_w = 24,063 g/mol, M_n = 23,618 g/mol, dn/dc = 0.132 ml/g, η = 0.4 dl/g) and dextran (T70K, M_w = 70,026 g/mol, M_n = 55,411 g/mol, dn/dc = 0.147 ml/g, η = 0.26 dl/g) were obtained from Malvern Instruments (Worcestershire, UK). The FastDNA™ SPIN KIT for soil was purchased from MPbio (Zurich, Switzerland). Water of MilliQ quality, H₂O; ≥18.2 MΩ cm at 25°C, was used for aqueous solutions (Merck Millipore, Darmstadt, Germany).

Methods

Arabinoxylan Processing and Extraction

SwissMill (a division of the Coop cooperative, Basel, Switzerland) kindly provided the native and extruded WB from *Triticum aestivum*. Milled WB sample material was additionally produced by ultra-centrifugal milling for the simulation of mechanical processing. For this purpose, a ZM200 ultra centrifugal mill (Retsch GmbH, Hann, Germany) was equipped with a 12-teeth rotor and a sieve with trapezoid holes of 0.5 mm. The Technical Research Centre of Finland (VTT Finland) kindly provided the native and extruded RF. Water-extractable arabinoxylan was extracted from the sources mentioned above using a previously published method (15). The freeze-dried material of multiple extractions was pooled and pulverized in a ball mill equipped with a 15-ml grinding bowl and two steel balls with a diameter of 15 mm for 1 min.

To compare the influence of impurities of AX extracts on the prebiotic potential, both wheat and rye fermentations were additionally performed with a commercial wheat and rye AX standard, namely, WAX and RAX, respectively. In both cases, Fenton oxidized WAX and RAX, namely, OXWAX and OXRAX, were additionally produced to simulate food processing-induced structural modification (30). For this purpose, WAX or RAX (132 mg) was dissolved in H₂O (5 ml) for 1 h at 80°C and stirred at 20°C overnight. Following that, 50 μM FeSO₄, 50 μM ascorbic acid, and 50 mM H₂O₂ were added in this order to give a final concentration of 2% AX (w/v). The Fenton oxidation was heated for 3 h at 80°C, then continued at room temperature with access to air for 24 h. The oxidation was done in triplicates and subsequently freeze-dried and pulverized analogously to the extracts. Structural features of both standards and the respective oxidized standard are shown in the **Table 1**.

Extract and Monomeric Sugar Composition

The monomeric sugar composition of the extracts was determined according to Demuth et al. (15) by high-performance anion-exchange chromatography with pulsed amperometric detection (HPAEC-PAD) after hydrolysis with trifluoroacetic acid. The 10-mg sample materials were hydrolyzed with 2.5 ml 2 M TFA for 4 h at 100°C. The HPAEC-PAD separation was

based on a procedure by Hardy et al. (31) and Rohrer et al. (32) with modifications. A Dionex™ ICS-5000+ Capillary HPIC™ System with a Dionex™ CarboPac™ PA1 IC column (Thermo Fischer Scientific AG, Basel, Switzerland) maintained at 26°C was used. The injection volume was 10 μl and the flowrate was 1 ml/min. Eluent (A) consisted of water and eluent (B) had 200 mM of NaOH. The gradient started with 92% (A) for 20 min. After 20 min, the gradient was changed to 100% (B) for 10 min, and finally re-equilibrated for 8 min with 92% (A). For the pulsed amperometric detection, replaceable gold electrodes were used in waveform A adapted from the Dionex technical note 21. All samples were measured in quintuplicates. L-(+)-arabinose and D-(+)-xylose as well as D-(+)-glucose and D-(+)-galactose were externally calibrated using a 13-point calibration from 1.25 to 100 μg/ml with 10 μg/ml of D-(-)-sorbitol as internal standard. Data processing was done in Chromeleon 7 (Thermo Fischer Scientific AG, Basel, Switzerland).

Nitrogen Content

Elemental nitrogen (% N) content in the extracts was quantified in triplicates using a Flash EA 1112 Series elemental analyzer (Thermo Italy, former CE Instruments, Rhodano, Italy) coupled to a Finnigan MAT Delta^{plus} XP isotope ratio mass spectrometer (Finnigan MAT, Bremen, Germany) as described by Werner et al. (33) and Brooks et al. (34). Subsequently, the protein content was calculated using a conversion factor of 5.7 for grains (35).

Phenolic Acid Determination

The bound phenolic acids were determined in quadruplicates by reversed-phase high performance liquid chromatography (RP-HPLC) with an ultraviolet detector (UV) as published earlier (15) using 10 mg of AX extracts. The eluted phenolic acids were detected at 254, 280, and 325 nm and processed by Chromeleon 7 (Thermo Fischer Scientific AG, Basel, Switzerland).

M_w Analysis

The weight average molecular weight (M_w) of the AX extracts was determined using high performance size exclusion chromatography (HPSEC) coupled with triple detection (15). The system consisted of OMNISEC resolve (OMNISEC, Malvern Panalytical Ltd., Malvern, United Kingdom) coupled to the multi-detector module OMNISEC reveal (OMNISEC, Malvern Panalytical Ltd., Malvern, United Kingdom) including an RI, RALS (90°), LALS (7°), and a VISC detector. Two A6000M columns with an exclusion limit of 20,000,000 g/mol (Malvern Panalytical Ltd., Malvern, UK) were maintained at 35°C with a flowrate of 0.7 ml/min using an aqueous mobile phase with 0.1 M NaNO₃/0.02% NaN₃. The injection volume was 100 μl, and the elution was recorded for 42 ml. Polyethylene oxide calibration standard (2.498 mg/ml, dn/dc 0.132 ml/g, M_w 23.85 kg/mol) and dextran verification standard (2.433 mg/ml, dn/dc 0.148 ml/g, M_w 70.03 kg/mol) solutions were prepared in an aqueous solvent with 0.1 M NaNO₃/0.02% NaN₃. Arabinoxylan isolates were dissolved equally by heating them to 80°C under constant stirring for 30 min, with a final concentration of 1 mg/ml. Subsequently, the samples were stirred overnight at 20°C and filtered using

TABLE 1 | Structural features of differently processed wheat bran (WB) and rye flour (RF) arabinoxylan (AX) and wheat and rye AX standards (WAX, RAX) as well as the respective oxidized standard (OXWAX, OXRAX)[†].

	Native WBAX	Milled WBAX	Extruded WBAX	Native RFAX	Extruded RFAX	WAX	OXWAX	RAX	OXRAX
M _w [kg/mol]	403 ± 41 ^a	134 ± 11 ^b	345 ± 21 ^a	234 ± 18 ⁱ	520 ± 50 ⁱⁱ	330	6.28 ± 0.08	440	10.2 ± 0.1
Arabinoxylan [mg/g]	415 ± 10 ^a	563 ± 30 ^b	463 ± 42 ^c	480 ± 11 ⁱ	540 ± 21 ⁱⁱ	950	950	900	900
Arabinose [mg/g]	135 ± 3 ^a	173 ± 10 ^b	141 ± 15 ^a	134 ± 7 ⁱ	161 ± 09 ⁱⁱ	N/A	N/A	N/A	N/A
Xylose [mg/g]	280 ± 6 ^a	391 ± 20 ^b	322 ± 28 ^c	330 ± 12 ⁱ	370 ± 19 ⁱⁱ	N/A	N/A	N/A	N/A
A/X ratio	0.483 ± 0.002 ^a	0.441 ± 0.005 ^b	0.436 ± 0.008 ^c	0.41 ± 0.01 ⁱ	0.44 ± 0.01 ⁱⁱ	0.61	0.61	0.61	0.61
Glucose [mg/g]	9.4 ± 1.1 ^a	5.7 ± 1.0 ^b	28.9 ± 3.4 ^c	2.10 ± 0.20 ^j	5.2 ± 0.3 ⁱⁱ	N/A	N/A	N/A	N/A
Galactose [mg/g]	10.3 ± 0.3 ^a	6.4 ± 0.2 ^b	4.4 ± 0.4 ^c	–	–	N/A	N/A	N/A	N/A
Protein [mg/g]	50.7 ± 0.2 ^a	49.3 ± 1.7 ^a	48.9 ± 0.5 ^a	24.0 ± 0.8 ^j	14.0 ± 1.0 ^j	N/A	N/A	N/A	N/A
Bound phenolic acids [mg/g]	2.4 ± 0.7 ^a	4.0 ± 1.0 ^b	4.0 ± 0.7 ^b	6.0 ± 0.6 ⁱ	6.67 ± 1.07 ⁱ				

An in-depth characterization of the WBAX was published earlier (15).

[†]Note that letters indicate significant differences corresponding to $\alpha = 0.05$ among the differently processed samples, compared means were native, milled, and extruded WBAX as well as native and extruded RFAX.

0.45- μ m nylon filters. The system was calibrated with a one-point calibration approach using a narrow PEO standard with known parameters. The samples were measured in triplicates and the data evaluation was performed with the Malvern software OMNISEC V10.30. The refractive index increment (dn/dc) of 0.132 ml/g was determined by HPSEC using WAX and RAX as AX reference standards.

In vitro Colon Fermentation of AX

The fermentation of various soluble WBAX and RFAX by colon microbiota was determined by an *in vitro* colon high-throughput batch fermentation using two different *in vitro* cultivated proximal colon microbiota (CM 1 and CM 2). The focus of this study was on the impact of processing-induced structural changes of AX on its colonic fermentation; therefore, the hydrochloric acid predigestion of extracts prior to the fermentation was not performed as it may have additionally modified the structure of AX, preventing the direct processing-structure-function correlation (36). The microbiota were derived from two independent stable PolyFermS systems, a continuous colon fermentation model, which were inoculated with the immobilized fecal microbiota of healthy human adults and are designed to continuously cultivate the proximal colon microbiota akin to donor profile (37, 38). The fecal samples for initiating the PolyFermS system were donated by two healthy individuals (females, aged 27 and 28) with Western-style diets who did not receive any antibiotics or probiotics for at least 3 months before donation. The Ethics Committee of ETH Zürich exempted this study from review because the sample collection procedure was not performed under conditions of intervention. Informed written consent was obtained from the fecal donors. The donor fecal and *in vitro* cultivated proximal colon microbiota profile is provided in the (Supplementary Table 1).

In vitro colon microbiota fermentations were performed in a Macfarlane-based medium for the cultivation of the human colon microbiota (39). A double-concentrated Macfarlane medium without fibers containing 3 g/L ampicase, 5 g/L Bacto™ tryptone, 1.5 g/L meat extract, 4.5 g/L yeast extract, 4 g/L mucine

from porcine stomach, 0.4 g/L bile salt, 3 g/L potassium dihydrogen phosphate, 9 g/L sodium bicarbonate, 4.5 g/L sodium chloride, 4.5 g/L potassium chloride, 0.65 g/L magnesium sulfate, 100 mg/L calcium chloride, 200 mg/L manganese chloride, 5 mg/L iron sulfate, 100 mg/L zinc sulfate, 5 mg/L, and 5.7 ml/L (v/v) of a volatile fatty acid mix (acetate, propionate, isovalerate, isobutyrate, valerate) with a pH of 6.8 was prepared (40).

The media were filled anaerobically into serum flasks, sealed, and then autoclaved. A sterile-filtered vitamin solution was added to the medium prior to the experiment (41). Predigesting of the evaluated AX extracts was generally prevented to exclude any additional structural modifications to the one induced by processing. The AX solutions were heated to 80°C for 30 min, stirred overnight, and filter sterilized using 0.22 μ m PTFE filters (BGB Analytik AG, Boeckten, Switzerland). Subsequently, AX solutions were added to the media to obtain a final concentration of 5 mg/ml AX and a normal concentrated Macfarlane medium (39). The determined AX purities of the different AX extracts were considered in the preparation of AX solutions targeting a final concentration of 5 mg/ml in all AX solutions (see Table 1 AX content). The investigated dose (5 mg of soluble AX/ml) mimics a dietary intake of 1 g of soluble AX/day when taking into account the average volume of the proximal colon (200 ml (42)) and assuming no upper digestive tract AX degradation and uptake. This dose is within the range of a Western human adult diet based on an average whole grain intake of 50 g/day (43) and a soluble AX content of approximately 2.2% (10) or up to 1–2% (10, 15) in rye flour or wheat bran, respectively.

The mixture of fiber and medium solution was added to 24-well plates and inoculated with an *in vitro* cultivated proximal colon microbiota at an inoculation rate of 1% (v/v) and final fermentation volume of 2 ml. A negative control was included consisting of a fiber-free Macfarlane medium. All manipulations were done in an anaerobic tent (10% CO₂, 5% H₂, 85% N₂) (Coy Laboratories, MA, USA) and the well-plates were incubated anaerobically for 0, 6, 12, 24, or 48 h at 37°C in the dark. Each treatment per *in vitro* colon microbiota and per time point was performed in technical quadruplicates. At each time point,

fermentation of one 24-well plate was stopped and sampled for pH, SCFA, and bacterial quantification.

The fermentation kinetics was assessed by pH measurement and SCFA quantification over time and correlated with changes investigated in bacterial growth and composition at 12 h and 24 h.

SCFA Quantification

The fermentation metabolites acetate, propionate, butyrate, isobutyrate, lactate, succinate, valerate, iso-valerate, and formate were quantified. Therefore, an aliquot of 1 ml at each sampling point was centrifuged (13,000 cfm for 10 min at 4°C) and the supernatant was then filtered using an 0.45 µm PTFE (Phenomenex Helvetia GmbH, Basel, Switzerland) filter. The samples were then analyzed using an HPLC (Merck-Hitachi, Selm, Germany) equipped with a Cation-H refill cartage (Bio-Rad Laboratories AG, Reinach, Switzerland) (30 × 4.6 mm) connected to an Aminex[®] (Bio-Rad Laboratories AG, Reinach, Switzerland) HPX-87H (300 × 7.8 mm) column and a refractive index detector (Thermo Fisher Scientific AG, Pratteln, Switzerland). The injection volume was 40 µl. The mobile phase used was 10 mM H₂SO₄ with a flow rate of 0.6 ml/min at 40°C under isocratic conditions. The metabolites were quantified by external calibration.

Microbial Community Analysis

The microbial community was analyzed by qPCR and Illumina next generation 16S rRNA gene amplicon sequencing. The analysis was carried out on randomly selected technical triplicates or all quadruplicates from timepoints 12 and 24 h. Genomic DNA was extracted from the pellet of 1 ml of the fermentation sample and performed according to the procedure of the FastDNA[™] SPIN KIT for soil purchased from MPbio (Zurich, Switzerland). Total DNA concentration (ng/µl) and purity were determined by spectrophotometry using the Nanodrop (Nanodrop ND 1000, Thermo Scientific, Wilmington, DE, USA). Then, the DNA extracts were diluted to a DNA concentration of 20 ng/µl in nuclease-free molecular grade water and stored at 4°C until any further downstream analysis.

Quantitative real-time PCR of the 16S rRNA gene for total bacteria [primer Eub338F and Eub518R), *Lactobacillus/Leuconostoc/Pediococcus* (primer F_Lacto 05, F_Lacto 04)], and *Bifidobacteria* (primer Bif F and Bif R) were performed in triplicates (44–46). The qPCR assays were performed in triplicates in 10 µl using 2 µl of diluted genomic DNA, 5 µl of 2X SensiFast SYBR No-ROX Mix (Bioline, Luckenwalde, Germany), and 500 nM of each forward and reverse primer. The analysis was performed in a Roche LightCycler 480 II (Roche Diagnostics, Rotkreuz, Switzerland). Reactions were pre-incubated at 95°C for 3 min, followed by 45 cycles at 95°C for 5 s and 60°C for 30 s, and then a melting curve analysis. For quantification, a dilution series of standards was obtained by amplification of the linearized plasmids containing the gene of a representative bacterial species belonging to the target group and included in each run. Primer specificity and verification of the presence of the desired amplicon were determined by melting curve analysis. The PCR efficiency (%) was calculated from the slope of the standard curve of each qPCR

assay. Assays with an efficiency of 80–110% (slope of 3.2–3.9) were included in the data analysis. The gene copy number of the qPCR results were transferred to numbers of bacteria/ml by correcting for the median 16S rRNA gene copy number based on the Ribosomal RNA Database (47).

The microbiota community profiling was performed using 16S rRNA gene amplicon sequencing by StarSEQ (Mainz, Germany). The bacterial compositions of the differently treated WBAX and RFAX samples from timepoints 12 and 24 h were determined using tag-encoded 16S rRNA gene MiSeq-based (Illumina, CA, USA) high-throughput sequencing. The V4 region of the 16S rRNA gene was amplified with modified primers, namely, 515 F (TATGGTAATTGTGTGNCAGCMGCCGCGGTAA) and 806 R (AGTCAGTCAGCCGACTACHVGGGTWTCTAAT). One MiSeq cell and the V2 2 × 250 bp paired end Next Tera chemistry supplemented with 20% of PhiX was utilized.

The raw sequence data have been submitted to European Nucleotide Archive (ENA) database with accession number PRJEB44740. Raw data were processed using the DADA2 R package [version 1.14.1, (48)] to obtain exact amplicon sequence variants (ASVs). Forward and reverse reads were truncated after 170 and 160 nucleotides, respectively. After truncation, reads with expected error rates higher than three and four for forward and reverse reads, respectively, were removed. After filtering, error rate learning, ASV inference, and denoising, reads were merged with a minimum overlap of 40 bp. Chimeric sequences were identified and removed. Taxonomy was assigned to ASVs using DADA2 against the SILVA database (v138) (49). The open-source bioinformatics pipeline Quantitative Insight Into Microbial Ecology (QIIME2) was used for subsequent analysis, including alpha and beta diversity (50).

Statistical Analysis

The ANOVA one-way statistical analysis with a significance level of 0.05 was performed to identify significant differences between means in structural analysis and SCFA concentration considering the assumptions required for parametric testing. *Post-hoc* analysis was carried out using Tukey HSD in Origin pro 2019 (OriginLab Corporation, MA, USA). Comparisons were performed among differently processed extracts and between oxidized and non-oxidized standards. Pairwise Kruskal–Wallis analysis was performed on alpha diversity metrics to identify significant differences between treatments in QIIME2. Permutational multivariate ANOVA (PERMANOVA) was performed based on weighted and unweighted UniFrac distance matrices followed by pairwise tests to identify the significant differences between treatments in QIIME2. To identify the significant differences in genus composition between treatments after 12 or 24 h fermentation, the DESeq2 method was applied with the DESeq and phyloseq package (51, 52) in R, version 4.0.4 (53).

RESULTS

This study was designed to investigate the effect of grain milling and extrusion on the *in vitro* colon microbiota fermentation

of soluble AX isolated from WB and RF. Soluble AX was extracted from native, milled, and extruded WB, and from native and extruded RF. Furthermore, commercially available soluble AX standards originating from RAX and WAX were incorporated in all experiments to exclude the side effects of impurities in the generated extracts. In addition, these standards were Fenton oxidized to chemically simulate processing-induced modifications (OWAX and OXRAX). Finally, the naturally occurring and processing-induced structural changes of soluble AX were correlated with the fermentation behavior of two cultivated human colon microbiota (CM) to define a structure–function relation. For this purpose, the obtained AX extracts were characterized by the structural features M_w , sugar composition, arabinose to xylose (A/X) ratio, and bound phenolic acids content.

Structural Characterization of Differently Processed Soluble Arabinoxylan

In this study, M_w was determined by HPLC-RI/RALS/LALS/VISC. The M_w of native RFAX (234 ± 18 kg/mol) increased significantly by 100% through extrusion (520 ± 50 kg/mol) suggesting solubilization of insoluble AX (Table 1). In contrast, the extrusion of WB did not cause a significant change in M_w , while the milling of WB induced a significant M_w reduction from 403 ± 41 kg/mol (native WBAX) to 134 ± 11 kg/mol (milled WBAX). The Fenton oxidation caused a significant M_w degradation through chain scissions in both WAX and RAX (Table 1), while the oxidation of RAX reduced the M_w from 440 kg/mol to 10.2 ± 0.1 kg/mol and an even stronger degradation was observed for WAX from 330 kg/mol to 6.28 ± 0.8 kg/mol.

The monomeric sugar composition of the WBAX isolates was determined after complete hydrolysis by HPAEC-IPAD. The varying extract purity for AX was considered in the subsequent fermentation experiment. The arabinose substitution changed significantly through processing (Table 1). The solubilization of slightly branched high M_w AX during extrusion significantly increased the A/X ratio of rye flour from 0.41 ± 0.01 to 0.44 ± 0.01 . In contrast, the A/X ratio of native wheat bran AX decreased significantly through both milling and extrusion. Moreover, the degree of substitution varied significantly between WBAX and RFAX. Generally, native RFAX (0.405 ± 0.009) presented a lower A/X ratio than native WBAX (0.483 ± 0.002), which indicated a less substituted structure. The soluble AX extracted from all three WB samples contained both glucose and galactose, whereas RFAX samples only contained glucose. In both cases, extrusion increased glucose content significantly. However, the glucose concentration in RFAX was lower than in the WBAX samples, even after extrusion with maximal 5.2 ± 0.3 mg/g. The highest glucose content was found for extruded WBAX with 28.9 ± 3.4 mg/g, which is in line with a study of Ralet et al. (54), who found that extrusion enhances the glucoarabinoxylan solubilization from the pericarp layer of wheat. Wheat bran AX samples had equal galactose concentrations. The presence of galactose can be explained by the co-extraction of residual water-soluble arabinogalactanpeptides (55). We observed the release of galactose through bacterial enzymatic degradation during the

in vitro colon fermentation of WBAX, confirming the above structural data (data not shown).

The protein content among the extracts evaluated ranged between 1 and 5% in WBAX and RFAX. As a specific structural feature of AX, the total quantity of bound phenolic acid was determined in the extracts obtained. In general, RFAX contained significantly more bound phenolic acids than WBAX. For both sample types, processing increased the content of bound phenolic acids, which may be explained by the solubilization effect of high M_w AX with a rather complex molecular structure. However, it seems that extrusion partially degraded the liberated phenolics. Both ferulic and sinapic acid were the only two phenolic acids identified in the samples, whereas ferulic acid was dominated (data not shown).

In vitro Colon Microbiota Fermentation of Differently Processed AX

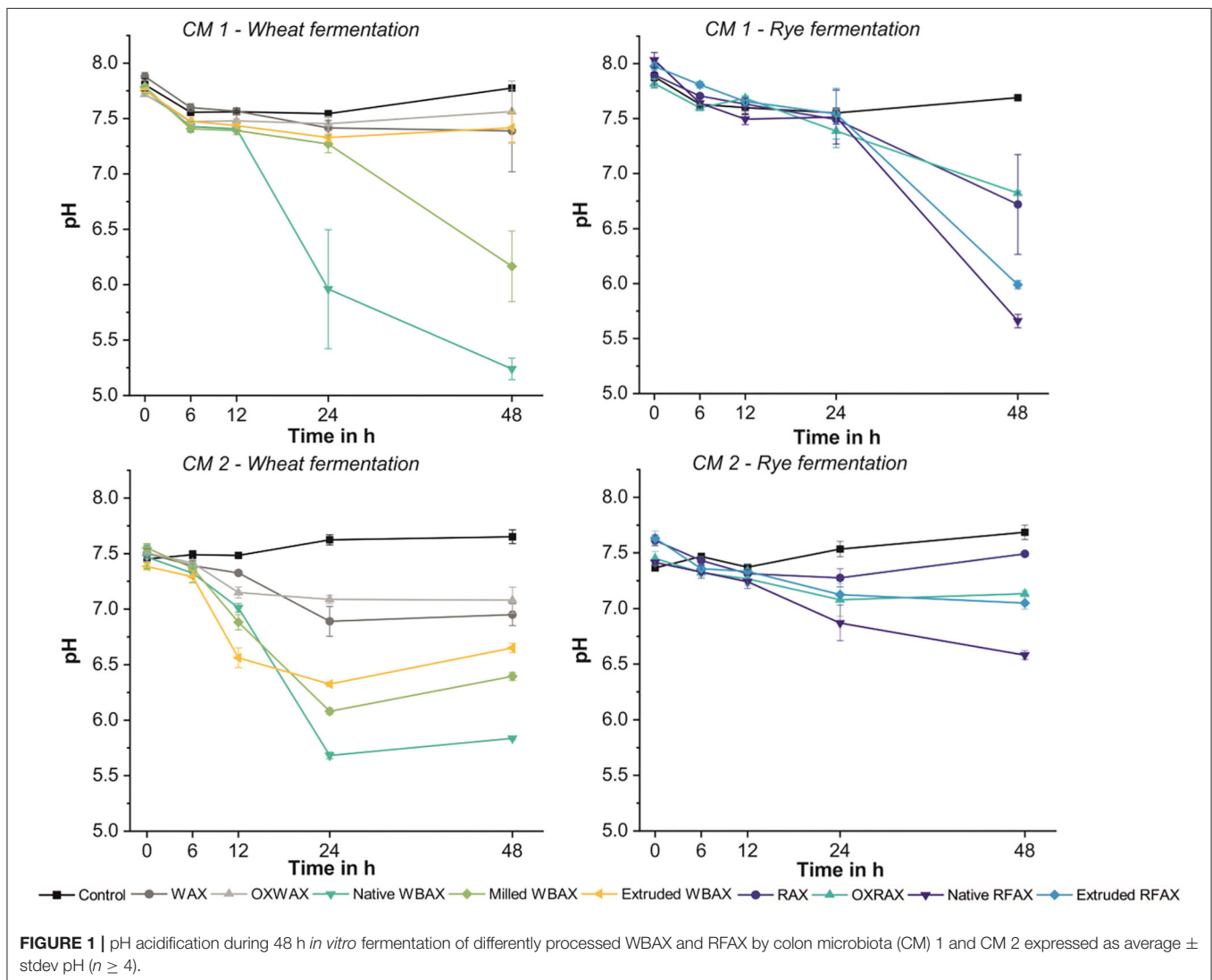
The *in vitro* colon microbial fermentation of the different soluble AX extracts was evaluated over 48 h by means of pH change, SCFA production, and microbial community profiling. The two cultivated microbiota (CM) were representative for a healthy human proximal colon microbiota and differed in abundant bacterial families (Supplementary Table 1). Cultivated microbiota 1 was characterized by high levels of *Prevotellaceae* (56%), *Lachnospiraceae* (17%), and *Ruminococcaceae* (9%) while CM 2 was characterized by high levels of *Bacteroidaceae* (39%), *Lachnospiraceae* (22%), and *Ruminococcaceae* (14%). The two complementary CMs fermented the differently processed AX samples at different rates and to different extents.

AX Source and Processing Impacted pH Acidification Kinetics

The pH kinetics revealed remarkable differences between the two AX sources, namely, RFAX and WBAX, and, more importantly, between the differently processed AX extracts (Figure 1). Generally, CM 1 presented a stronger acidification for both WBAX and RFAX than CM 2. In both fermentations, differently processed WBAX resulted in a stronger acidification than the RFAX. Commercial and oxidized AX standards incorporated in the experiment caused only a slight pH decrease compared to the extracts. Among the different treatments, both native RFAX and native WBAX showed the strongest acidification over 48-h fermentation with an average delta pH of -2.4 (CM 1) and -0.8 (CM 2) for RFAX and -2.5 (CM 1) and -1.6 (CM 2) for WBAX. The fermentation of milled WBAX resulted in a stronger pH decrease than extruded WBAX in both CMs. Interestingly, the extruded WBAX did not induce an acidification in CM 1 (delta pH of -0.2), while it did in CM 2 (delta pH of -0.7). Notably, the WBAX fermentation by CM 2 microbiota showed an increase in pH during the final fermentation period (24–48 h), which is an indication for completed carbohydrate fermentation followed by proteolytic fermentation and concomitant ammonia formation (56).

SCFA Production Varied Between Microbiota, AX Sources, and Processing Methods

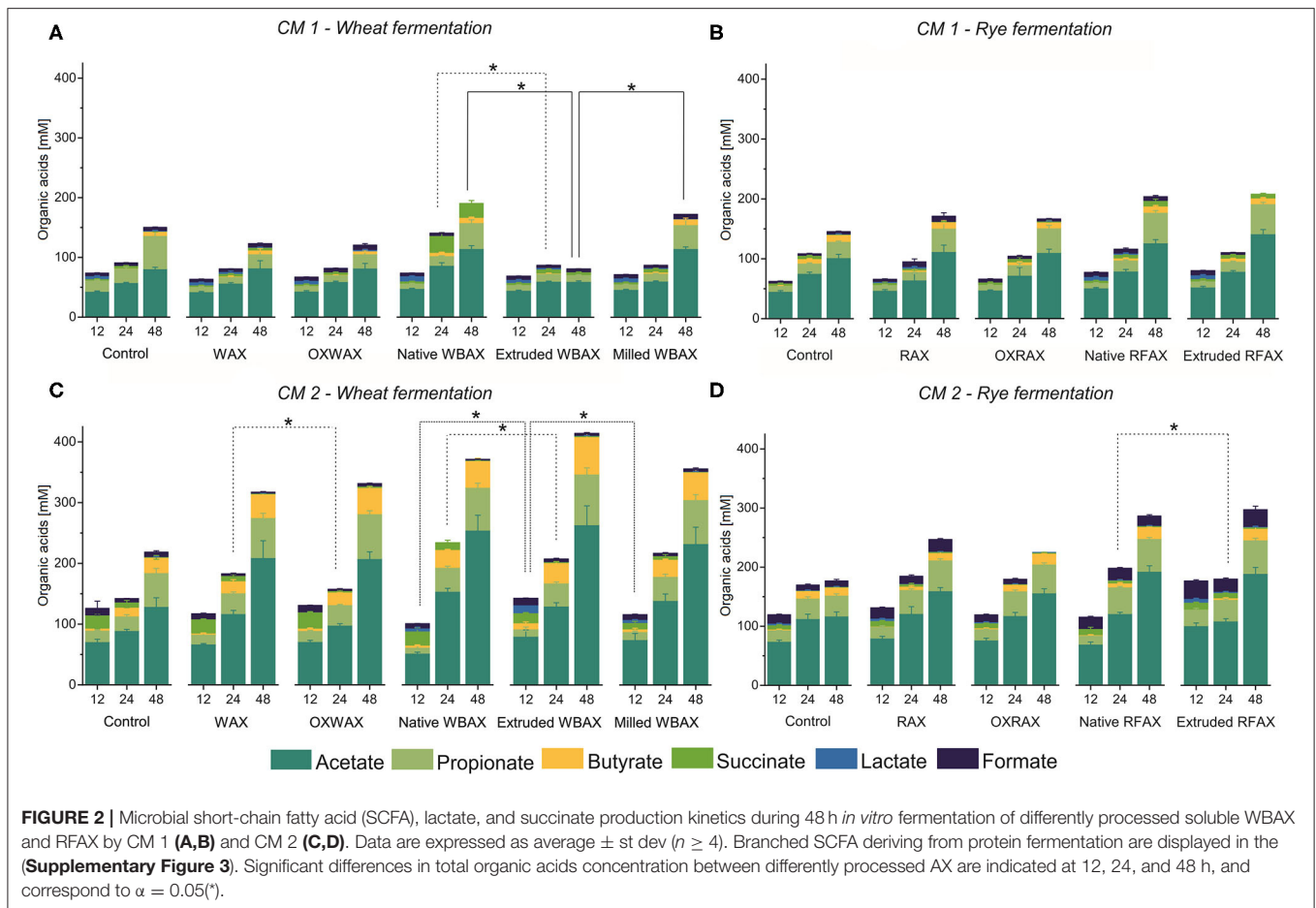
Overall, the metabolite levels increased during the 48 h fermentation in both CMs regardless of AX source and treatment



except for extruded WBAX in CM 1 (Figure 2). The SCFA acetate, propionate, and butyrate were the most abundant metabolites produced. Next to acetate, the main SCFA in CM 1 was propionate and, in CM 2, butyrate (Figure 3). The CM 2 microbiota generally produced more SCFA, lactate, and succinate than CM 1 microbiota with total levels ranging from 223.1 ± 10.4 (control) to 410 ± 50 mM (extruded WBAX) (Figures 2A,B) compared to 111 ± 12 and 196 ± 15 mM formed by CM 1 (Figures 2C,D). Moreover, the kinetics of the metabolite production and SCFA profile varied among the CMs evaluated. The majority of SCFA formed during the fermentation of WBAX and RFAX by CM 1 occurred after 24 h of incubation. In contrast, CM 2 produced significant SCFA levels already after 12 h of incubation. The enhanced fermentation rate by CM 2 is reflected in a faster acidification and a significantly higher SCFA formation combined with BCFA production observed for WBAX (Figure 1 and Supplementary Figure 3).

For the propiogenic CM 1 microbiota, differences in the production kinetics of intermediates (formate, lactate,

and succinate) and end metabolites (acetate, propionate, and butyrate) between WBAX and RFAX and among differently processed AX were observed (Figure 2 and Supplementary Figure 2). Generally, native WBAX induced a significantly higher production of end metabolites compared to extruded and milled WBAX. In particular, extruded WBAX showed little increase in end metabolites over time. Furthermore, the distinct production and conversion patterns of the intermediate metabolites formate, lactate, and succinate could be observed during the 48 h fermentation of the different WBAX samples. Native WBAX induced a high production of succinate (28 ± 5 mM) at 24 h compared to extruded and milled WBAX (6.8 ± 0.6 mM and 6 ± 0.7 mM, respectively). Both native and milled WBAX resulted in a slightly higher lactate production at 12 h (8.7 ± 0.3 mM and 6.5 ± 0.2 mM, respectively) compared to extruded WBAX (5.3 ± 0.2 mM). In contrast to the WBAX fermentation, the total end metabolite production of the native and extruded RFAX fermentations were comparable (Figure 2B). However, distinct differences in



metabolite composition were detectable over the progressing fermentation. During the fermentation of extruded RFAX, formate was faster metabolized or less accumulated than in native RFAX. Noteworthy, butyrate production was slower with RFAX samples compared to the negative control medium fermentation. Furthermore, differently processed WBAX and RFAX induced differences on the SCFA profile at 24 h, and WBAX also at 48 h (Figure 3A). Compared to native and milled WBAX, extruded WBAX resulted in relatively less propionate and butyrate at 48 h.

For the butyrogenic CM 2 microbiota, both WBAX and RFAX induced higher metabolite production compared to the control (Figures 2C,D). Differences in the production kinetics of intermediates (formate, lactate, and succinate) and end metabolites (acetate, propionate, and butyrate) between WBAX and RFAX and among differently processed AX were observed (Figure 2 and Supplementary Figure 2). Among all tested AX, the WBAX samples had the greatest effect on metabolic activity, leading to a strong formation of butyrate at the end of the fermentation, with the highest butyrate production with extruded WBAX (Figure 3B and Supplementary Figure 2). Similar to the findings of CM 1, native WBAX showed higher succinate accumulation at 12 and 24 h compared to extruded and milled WBAX (12 h: native 23 ± 6 mM; extruded: 16.6 ± 0.4 mM; milled: 11 ± 2 mM). Compared to native

and milled WBAX, extruded WBAX resulted in a higher lactate concentration at 12 h, which was metabolized at 24 and 48 h. Interestingly, extruded WBAX induced a faster and higher butyrate production by CM 2 compared to native and milled WBAX (Supplementary Figure 2). In contrast to WBAX, the RFAX fermentation resulted in lower amounts of metabolites with the accumulation of formate and lower butyrate levels (Figures 2D, 3B). Moreover, formate accumulation was higher with extruded RFAX compared to native RFAX at all timepoints (12 h: 29.9 ± 1.7 mM and 19.6 ± 1.4 mM, respectively).

In sum, the considerable variations in metabolite production between differently processed AX, especially observed for WBAX, in both CMs, indicate that the structural AX characteristics impacted the fermentation behavior.

Changes in the Microbial Community Through Differently Processed AX Fermentation

Variations in Microbial Composition Between Microbiota, AX Source, and Processing Method

The microbiota after 12 and 24 h of fermentation of differently processed WBAX and RFAX were analyzed using 16S rRNA gene amplicon sequencing. Samples of standard and oxidized standard AX were not included.

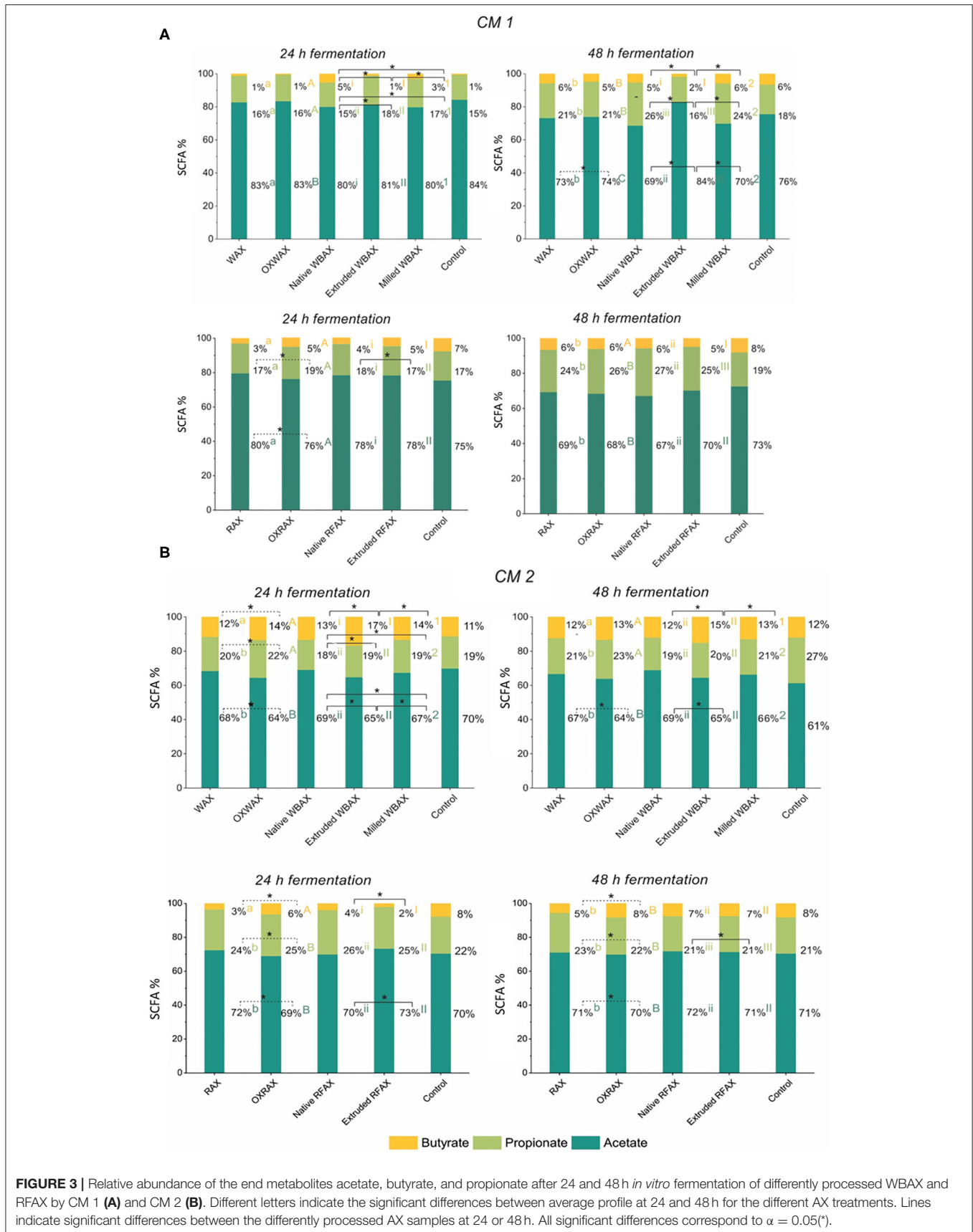


FIGURE 3 | Relative abundance of the end metabolites acetate, butyrate, and propionate after 24 and 48 h *in vitro* fermentation of differently processed WBAX and RFAX by CM 1 (A) and CM 2 (B). Different letters indicate the significant differences between average profile at 24 and 48 h for the different AX treatments. Lines indicate significant differences between the differently processed AX samples at 24 or 48 h. All significant differences correspond to $\alpha = 0.05$ (*).

The bacterial alpha diversity between the differently processed AX treatments was comparable within each microbiota after *in vitro* fermentation (Supplementary Figure 4). The beta diversity, which gives the variation in microbiota composition between samples, was evaluated to reveal differences of the microbial community between CMs, AX sources, and between differently processed AX. In general, the *in vitro* colon microbiota composition differed between CMs as indicated in a principle coordination analysis (PCoA)-biplot on weighted and unweighted UniFrac distance (Supplementary Figure 5). Furthermore, clear differences in the *in vitro* microbiota composition between RFAX and WBAX fermentation within both CMs were observed in unweighted and weighted UniFrac PCoA-biplots (Figure 4). The PERMANOVA analysis did not detect differences between differential processed AX for the unweighted UniFrac metrics except for CM 2, where extruded RFAX samples differed from native RFAX at 24 h ($p < 0.05$; Figure 5). When considering the ASV abundance, which is given by the weighted UniFrac distance, the PERMANOVA analysis detected differences between differently processed WBAX and RFAX at 12 and 24 h in both CM 1 ($p < 0.1$) and CM 2 ($p < 0.05$; Figure 5). In the case of CM 1, WBAX showed distinct clusters depending on the treatment after 24 h of fermentation, whereas RFAX exhibited strong variations after 12 h (Figures 5A,B). The microbiota of CM 2 showed differences after 12 and 24 h for the fermentation of differently processed WBAX and RFAX (Figures 5C,D). These assembled data suggest that the microbial composition and, in particular, the abundance of detected bacterial taxa depends on the AX source and the processing method indicating the influence of structural characteristics.

Consistently, the evaluation of abundant bacterial genera in the community revealed distinct differences between AX sources in their relative abundance (Figure 6 and Supplementary Figure 6; Supplementary Table 10). In both microbiota, after 24 h of fermentation, WBAX resulted in a higher abundance of *Blautia* and decreased abundance of *Enterococcus* and *Bacteroides* compared to control. In contrast, RFAX specifically enhanced the abundance of *Bacillus* and *Acinetobacter*, while lowering the abundance of *Agathobacter* when compared to control. Besides general effects on the microbial composition observed in both CMs, AX source also induced microbiota specific changes. The WBAX, for example, led in CM 1 to strong increases in abundance of *Bacillus*, *Paraprevotella*, and *Alloprevotella*, while in CM 2, it resulted in the increased abundance of *Faecalibacterium* and *Lachnospiraceae* genera compared to control ($|\text{Log}_2\text{FC}| > 3$, Supplementary Tables 7, 9).

The comparison between the differently processed WBAX and RFAX exhibited stronger $\text{Log}_2\text{FoldChanges}$ in genera present in CM 1 than in CM 2. Compared to native WBAX, processed WBAX resulted in CM 1 in lower abundances of the *Prevotella* and a *Lachnospiraceae* genera and higher abundance of *Enterococcus* and *Bacteroides* (Figure 6A and Supplementary Table 7). Type of WBAX processing also had an impact on the microbiota composition after fermentation. In CM 1, extruded WBAX led to a lower abundance of *Prevotella*, *Alloprevotella*, and *Lachnospiraceae* genera compared to milled

WBAX. Interestingly, the abundance of *Faecalibacterium* in CM 2 with extruded WBAX was lower after 12 h of fermentation but higher after 24 h of fermentation when compared to native and milled WBAX (Figure 6C and Supplementary Table 9). The compositional effects of RFAX processing were mainly detected after extrusion. Compared to native RFAX, extruded RFAX resulted in higher abundances of *Alloprevotella*, *Bacillus*, and *Solobacterium* and lower abundances of *Agathobacter* in CM 1 (Figure 6B and Supplementary Table 8). While in CM 2, extruded RFAX led to lower abundances of *Coprococcus*, *Dorea*, and *Blautia* compared to native RFAX (Figure 6D and Supplementary Table 10).

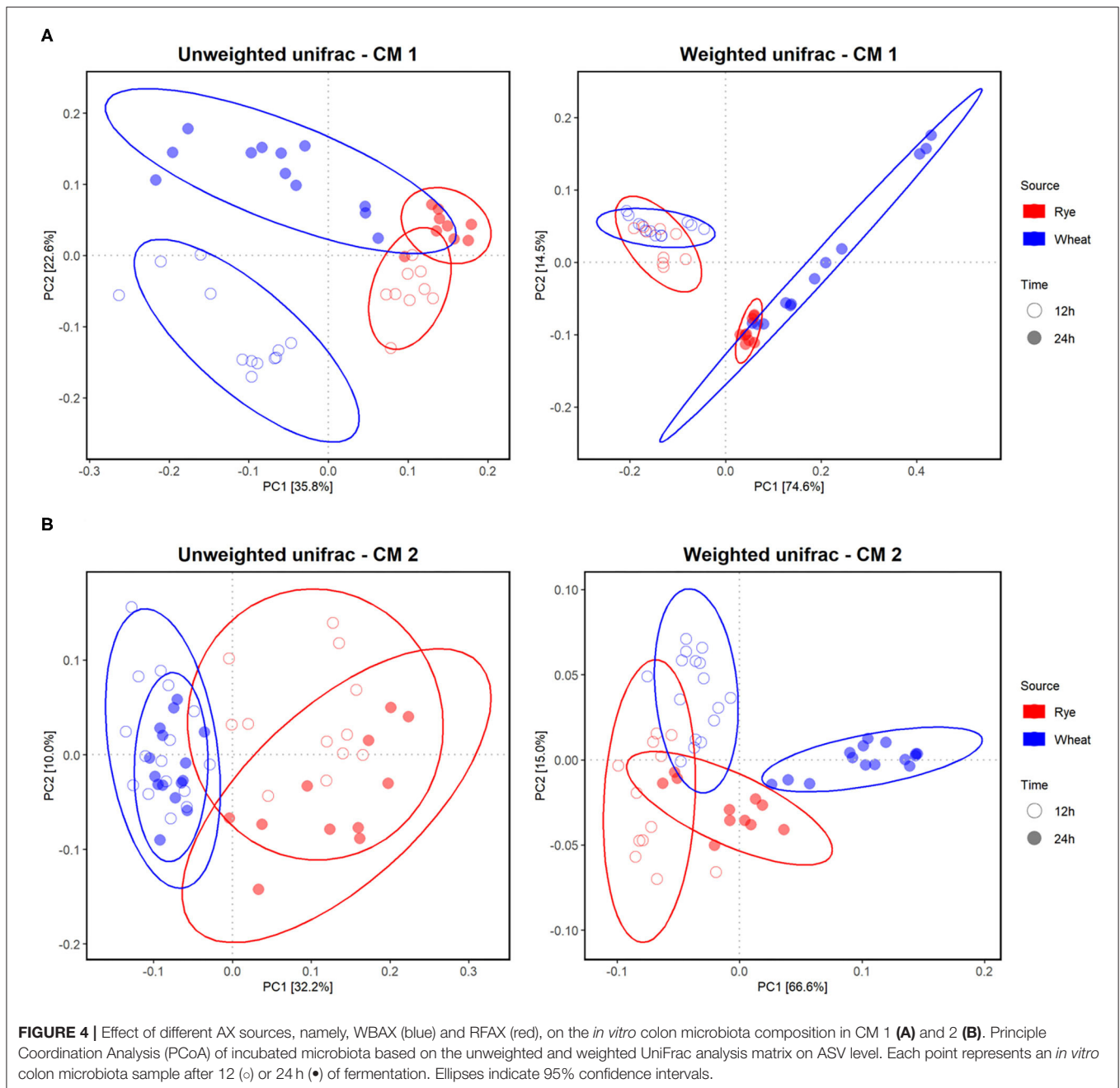
Differences in Total Bacteria, *Lactobacillus*/*Leuconostoc*/*Pediococcus* and *Bifidobacteria* Concentrations Associated With Microbiota, AX Source, and Processing Method

Quantitative PCR targeting total bacteria, *Lactobacillus*/*Leuconostoc*/*Pediococcus* spp. (LLP) and *Bifidobacteria* spp. was performed to assess the microbial growth after 12 and 24 h of AX fermentation in the differently processed WBAX and RFAX extracts (Figure 7).

In both microbiota, total bacterial growth was observed between 12 and 24 h of fermentation of AX, with higher end bacterial concentrations in CM 2 compared to CM 1 (Figure 7A). For both timepoints and CMs, RFAX did not promote the total bacterial growth compared to the control fermentation. Cultivated microbiota 1 (CM1) showed faster and higher growth with native WBAX (12 h: $3.5 \times 10^8 \pm 2.5 \times 10^7$ bacteria/mL) compared to extruded (12 h: $1.3 \times 10^8 \pm 1.2 \times 10^7$ bacteria/mL) and milled ($1.9 \times 10^8 \pm 1.7 \times 10^7$ bacteria/mL) WBAX. While CM 2, in contrast, showed faster bacterial growth with extruded and milled WBAX (12 h: $4.7 \times 10^9 \pm 4.0 \times 10^8$ and $3.1 \times 10^9 \pm 4.1 \times 10^8$ bacteria/ml, respectively) compared to native WBAX (12 h: $9.2 \times 10^8 \pm 1.1 \times 10^8$ bacteria/ml).

Native WBAX resulted in both microbiota in higher end concentrations of LLP compared to control fermentations (24 h, CM 1: $4.4 \times 10^6 \pm 3.8 \times 10^5$ vs. $3.4 \times 10^5 \pm 1.1 \times 10^5$ bacteria/ml, CM 2: $1.1 \times 10^8 \pm 2.0 \times 10^7$ vs. $4.4 \times 10^7 \pm 3.7 \times 10^6$ bacteria/ml) (Figure 7B). In contrast, processed WBAX resulted in lower LLP concentrations in CM 1 at 12 h fermentation, but higher LLP concentrations in CM 2 compared to native WBAX. RFAX did not promote the growth of LLP compared to the control fermentation and even resulted in lower end concentrations in CM 2, especially for extruded RFAX (24 h: $3.3 \times 10^7 \pm 2.5 \times 10^6$ vs. $1.7 \times 10^8 \pm 1.7 \times 10^7$ bacteria/ml) (Figure 7B).

The growth of *Bifidobacteria* spp. was stimulated by differently processed WBAX compared to control fermentation, especially in CM 2 resulting in higher *Bifidobacteria* concentrations compared to CM 1 after WBAX fermentation (24 h, CM 1: $4 \times 10^5 \pm 2.1 \times 10^4$ vs. CM 2: $7.8 \times 10^6 \pm 2.2 \times 10^6$ bacteria/ml) (Figure 7C). Compared to native WBAX, the extruded and milled WBAX induced a faster *Bifidobacteria* growth in CM 2 microbiota (12 h: native: $2 \times 10^5 \pm 4.7 \times 10^4$; extruded: $1.6 \times 10^6 \pm 9.8 \times 10^4$; milled: $7.2 \times 10^5 \pm 5.9 \times 10^4$ bacteria/ml) but not in CM 1 microbiota. The different RFAX samples did not



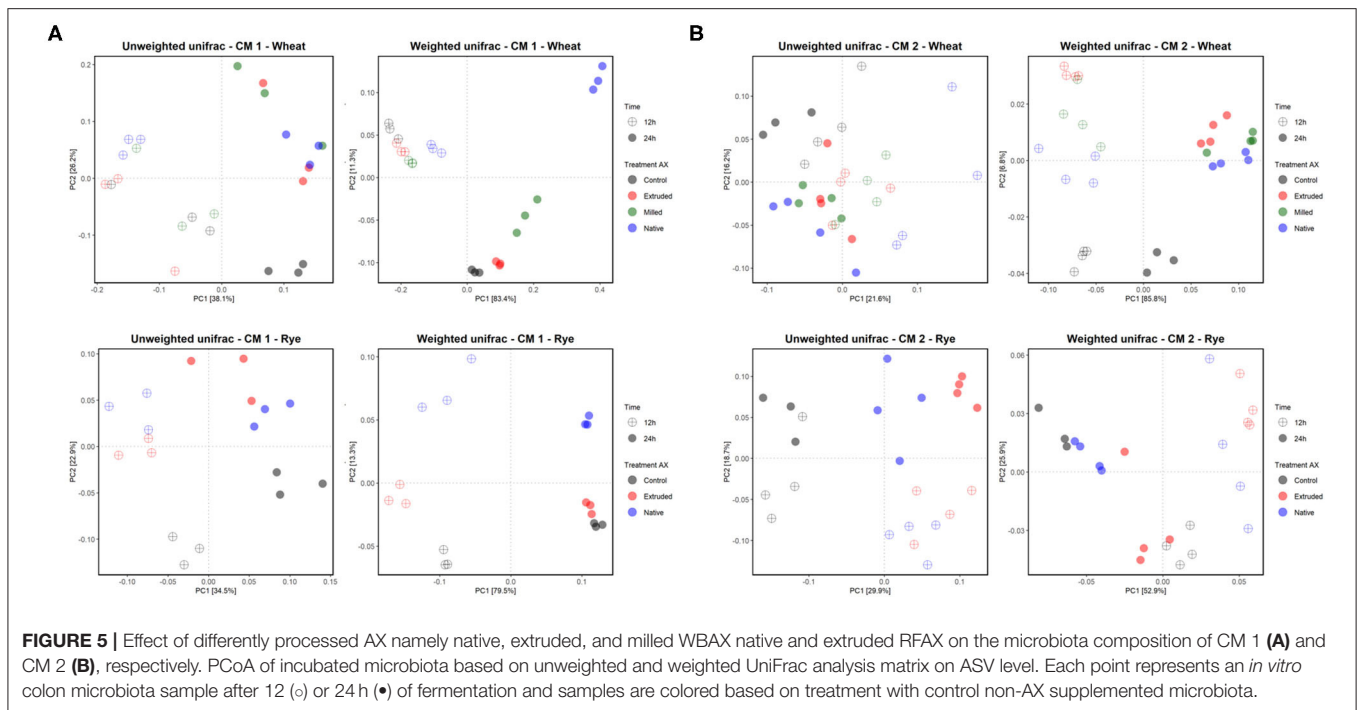
enhance the growth of *Bifidobacteria* compared to the control and even resulted in lower concentrations, as in the case of the extruded RFAX in CM 1 (24 h: $1.1 \times 10^5 \pm 4 \times 10^4$ vs. $2.6 \times 10^5 \pm 4.2 \times 10^3$ bacteria/ml) (Figure 7C).

DISCUSSION

The objective of this study was to evaluate the effects of naturally occurring and processing-induced structural alterations of soluble AX on the *in vitro* human colon fermentation. We hypothesized that fermentability and prebiotic potential would

improve with decreasing M_w and decreasing A/X ratio, and that these structural differences between wheat and rye AX and between differently processed AX would be reflected in SCFA production and the growth of health-associated taxa.

All differently processed WBAX and RFAX stimulated the production of SCFA, which is consistent with previous AX studies (57, 58). However, the extent of fermentation differed between AX fractions and source. RFAX showed a lower fermentability compared to WBAX. This implies that naturally given structural alterations such as the substitution pattern in wheat bran and rye flour AX affect their *in vitro* colon



fermentation behavior. This was also observed for rye, wheat, and oat bran (59) or AX isolated from corn, wheat, or rice brans (25, 60). Ultimately, further studies need to focus on a detailed structural characterization of differently processed AX derived from various grains.

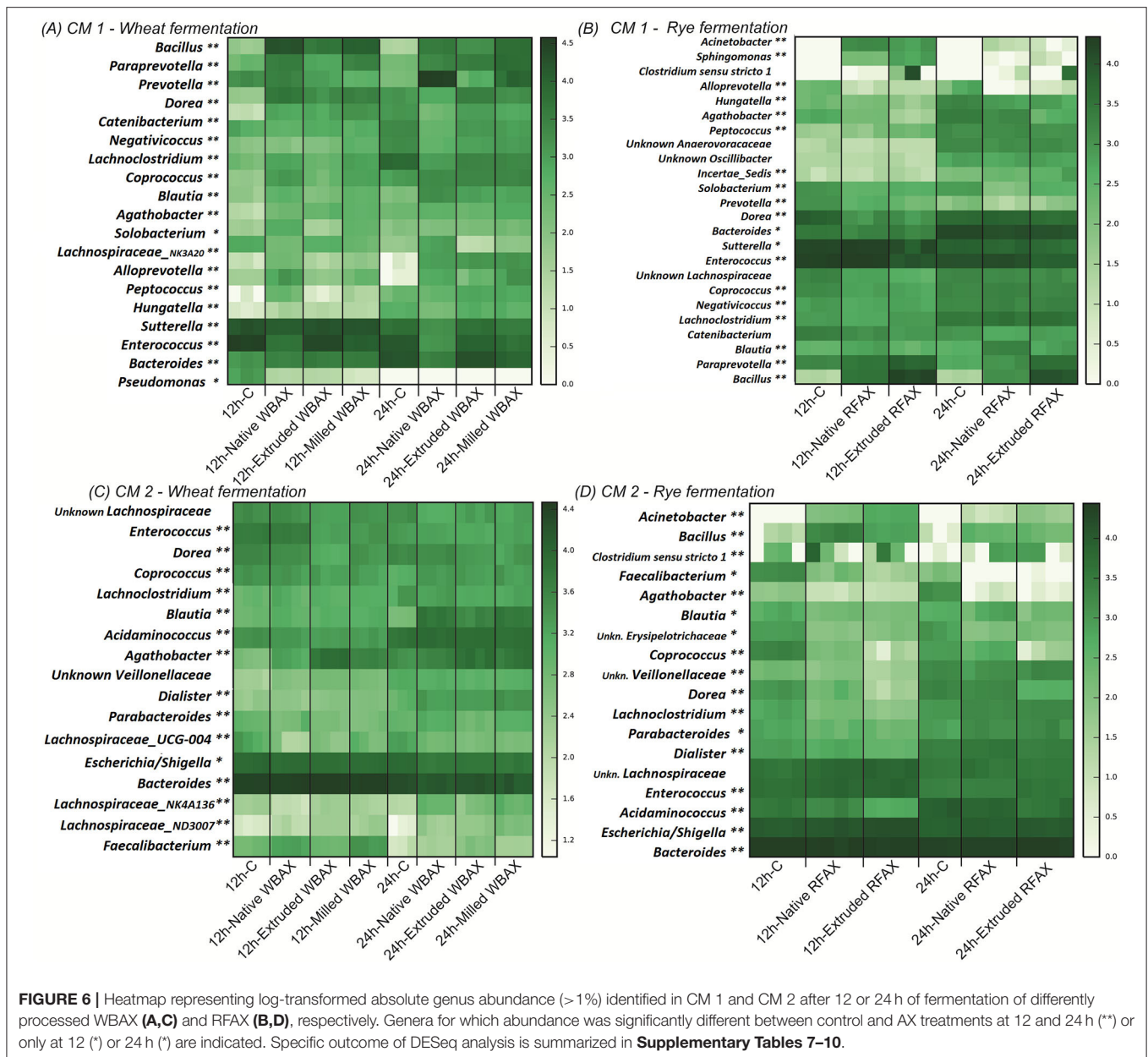
Native WBAX, which had the highest M_w and A/X ratio, showed the highest fermentability in both microbiota, while processed WBAX with lower M_w and a A/X ratio resulted in a lower acidification and SCFA production. These findings contradict the hypothesis of our study and previous studies, which suggest that low M_w improves AX fermentability because it facilitates the access of enzymes (20). Furthermore, the data show that there is no direct link between A/X ratio and the resulting fermentation behavior. This is in line with the observations made by Rumpagaporn et al. (25) who did not observe a correlation between molecular size, A/X ratio, and degree of substitution of AX and their fermentation rate by human fecal microbiota; instead, they observed that branching and high complex sidechains have a greater effect on the fermentation kinetics. Consequently, an in-depth structural investigation of linkage and substitution patterns by NMR or LC-MS, as already reported for AXOS, would be required to identify the governing structural features influencing the prebiotic potential of the differently processed WBAX and RFXAX (61, 62).

Our results suggest that the amount of bound phenolic acids in AX, which were much higher in RFXAX and increased by milling and extrusion in both cereals, may inhibit and slow down the AX fermentation. It was hypothesized by Snelders et al. (62) that bound phenolic acids such as ferulic acids may cause sterical effects, limiting the accessibility for AX degrading enzymes and consequently inhibiting AX fermentation. Moreover, the authors

reported that the antimicrobial properties of feruloylation inhibited AXOS fermentation, which may also explain the overall lower fermentability of the RFXAX compared to WBAX observed in this study. Interestingly, significant differences in SCFA production between AX treatments disappeared after 48 h, despite higher bound phenolic acid content, implying that any initial effect of bound phenolic acid content did not persist. This could be because, once the steric hindrance had been cleaved by ferulolyl esterase-producing bacteria, the extruded WBAX was more degradable due to its less dense structure.

The fermentation rate of WBAX differed between the *Prevotellaceae*- (CM 1) and the *Bacteroidaceae*- (CM 2) dominated microbiota. The CM 2 microbiota showed a stronger bifidogenic and butyrogenic response upon WBAX compared to CM 1, which is in line with previous findings *in vivo* (22, 63). This can be the result of cross-feeding reactions between bifidobacteria- and butyrate-producing WBAX responding to *Faecalibacterium* and *Lachnospiraceae* taxa (23, 64). In CM 1, WBAX promoted propionate production and the growth of *Prevotella*, which corresponds with a recent study in healthy elderly that identified the *Prevotella* genus as a driving factor in microbiota response to wheat bran AX (65). The bloom of *Prevotella* also explained the succinate accumulation especially observed in native WBAX in CM 1, as some *Prevotella* species appear to produce succinate preferentially over propionate (66).

The extrusion of WBAX enhanced the butyrate production and abundance of *Faecalibacterium*, a genus associated with health (67) in butyrogenic CM 2 but did not impact fermentation in CM 1. This may be because of the low abundance of *Faecalibacterium* in CM 1 and the observed growth inhibition of its main AX fermenting genus, *Prevotella*, during extruded



WBAX fermentation. Also, during milled WBAX fermentation, a lower succinate production combined with a decreased abundance of *Prevotella* was observed. The lower fermentability of processed WBAX by propiogenic CM 1 may be explained by their higher levels of bound phenolic acids compared to native WBAX and their described antimicrobial activity (68). Indeed, previous *in vitro* work showed that ferulic acid-rich fiber fractions slowed down fermentation and, subsequently, inhibited propionate production (69, 70) or resulted in more butyrogenic fermentation (71). Hence, the identified differences in abundant taxa and end metabolites highlight the strong influence of AX processing on the microbial community and fermentation.

One limitation of our work is that we did not incorporate an *in vitro* upper digestive tract pre-digestion of the AX extracts

prior to *in vitro* colonic fermentation. This was to avoid the potential loss of water-extractable AX during such *in vitro* pre-digestions (16, 28), which would complicate the comparison of the fermentation behavior of the differently processed AX. However, we cannot exclude that, *in vivo*, the upper digestive tract passage may impact the AX extracts and their consecutive colonic fermentation. For instance, it was demonstrated that hydrochloric acid treatments lead to the degradation of arabinose substitutions within the AX chains (36). Therefore, future *in vitro* studies could investigate if processing-induced changes in soluble AX and their prebiotic potential are preserved after upper digestive tract conditions. Another limitation of the study is that only two microbiota were studied. Although common AX-induced effects on fermentation behavior were observed,

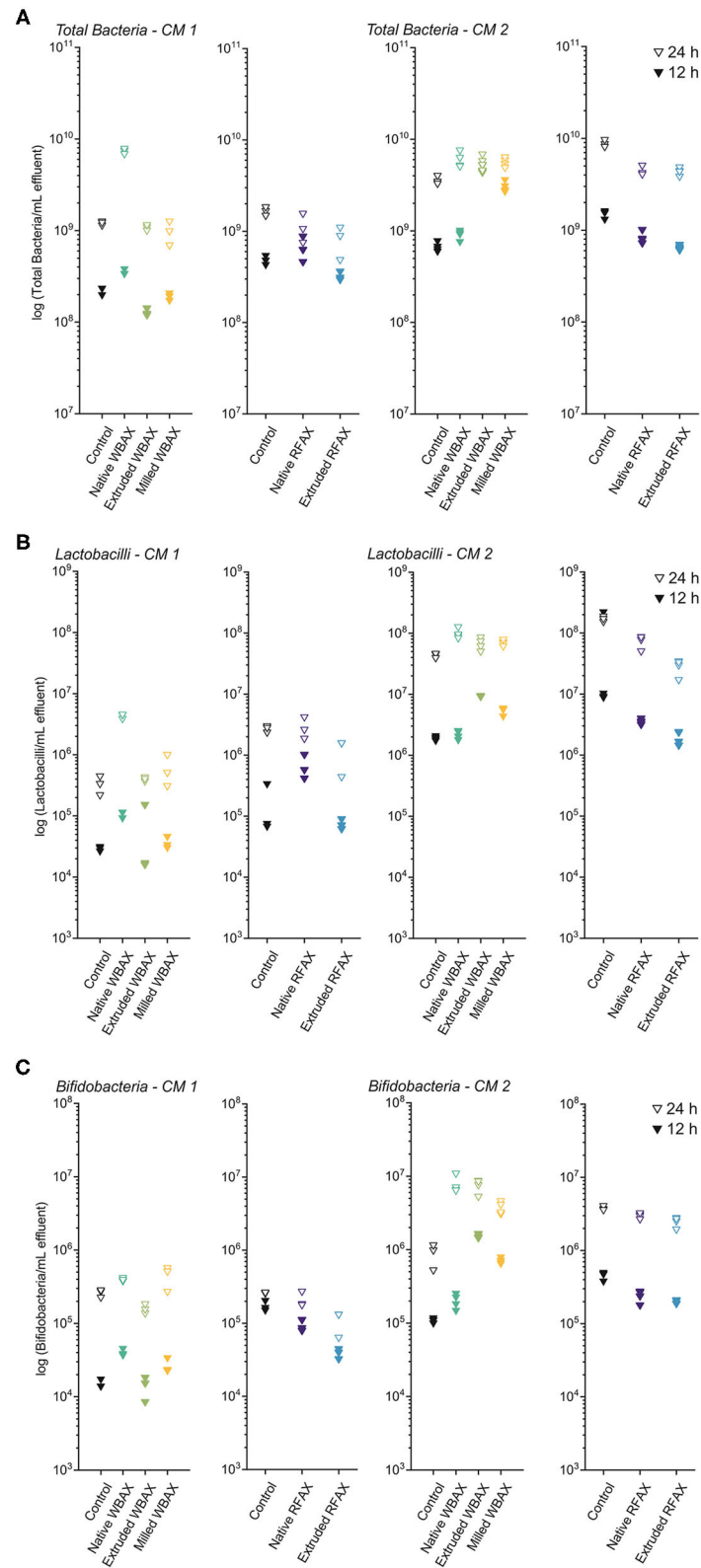


FIGURE 7 | Bacterial quantification by quantitative PCR targeting total bacteria **(A)**, *Lactobacillus/Leuconostoc/Pediococcus* spp. (LLP) **(B)**, and *Bifidobacterium* spp. **(C)** at 12 and 24 h of *in vitro* colon fermentation of differently processed WBAX and RFX by two CM 1 and CM 2.

several specific effects such as type of SCFA and type of bacterial taxa promoted differed between the microbiota. Several other *in vitro* studies with other types of wheat bran or AX extracts observed this individual microbiota response as well (26, 69, 72). In addition, data from human intervention studies often show very individual responses in microbiota change upon AX supplementation (24, 65), and their outcome is hard to predict due to the complex cross-feeding and ecological interactions occurring within the microbiota. The current setup is, therefore, a first step in gaining knowledge on the impact of processing-induced changes in soluble AX on fermentation kinetics and affected bacterial taxa but, obviously, there is a need for further investigation and validation with more individual microbiota *in vivo*. Such studies may allow for the selection of processing methods for producing AX fractions with different structural features and with predictable prebiotic shifts in gut microbiota (73).

CONCLUSION AND OUTLOOK

Prior research has often presented AX as a promising food constituent to prevent particular diet-related chronic diseases, which is associated with many beneficial effects resulting from its prebiotic activity. This study is the first report investigating the structure–function relation between naturally occurring and processing-induced structural alterations in soluble AX and its effect on *in vitro* colon fermentation.

The results demonstrate that fermentation behavior is strongly linked to the AX fine structure and their processing-induced modifications. The SCFA metabolism, acidification kinetics, bacterial growth, and bacterial composition revealed that wheat bran AX was fermented faster than rye flour AX. Extruded or milled AX did not enhance fermentation, nor did AX isolates with lower M_w and A/X ratio. High levels of bound phenolic acids were identified as an inhibiting factor for AX fermentation kinetics. Bacterial genera promoted by AX varied between AX source and processing type, but also between microbiota. Extruded WBAX promoted butyrate production and the growth of butyrate-producing *Faecalibacterium* in the butyrogenic microbiota but did not enhance fermentation in the propiogenic microbiota. These inter-individual differences highlight the particular importance to elucidate further individual responses to differently processed AX in future studies. Further investigations focusing on

the effect of processing-induced AX sugar functionalization or comprehensive linkage analysis are recommended, as well. This work provides the scientific framework for future *in vitro* fermentation and *in vivo* studies with processed dietary fibers.

DATA AVAILABILITY STATEMENT

The datasets presented in this study can be found in online repositories. The names of the repository/repositories and accession number(s) can be found below: <https://www.ebi.ac.uk/ena>, PRJEB44740.

AUTHOR CONTRIBUTIONS

TD, LN, and AG conceived the experiments. TD and VE conducted AX experiments and LB provided PolyFermS microbiota and data. TD, VE, and AG analyzed data and prepared figures. TD and AG wrote the manuscript and all authors reviewed the manuscript.

FUNDING

The study was funded by ETH Zurich and did not receive any specific grant from funding agencies in the public, commercial, or not-for-profit sectors.

ACKNOWLEDGMENTS

We gratefully thank Prof. Dr. Nesli Sözer and Dr. Markus Nikinmaa from VTT Finland for providing the rye flour samples used as an additional AX source. The authors thank Julia Isenring, Paola Morales, and Alfonso Die for technical support, and Dr. Florentin Constancias for support with the raw 16S data analysis. The authors thank Annika Ackermann from the Department of Environmental Systems Science at ETH Zurich for the protein determination. Part of this work was published in a doctoral thesis (<https://doi.org/10.3929/ethz-b-000451063>).

SUPPLEMENTARY MATERIAL

The Supplementary Material for this article can be found online at: <https://www.frontiersin.org/articles/10.3389/fnut.2021.707763/full#supplementary-material>

REFERENCES

- Putignani L, Del Chierico F, Petrucca A, Vernocchi P, Dallapiccola B. The human gut microbiota: a dynamic interplay with the host from birth to senescence settled during childhood. *Pediatr Res.* (2014) 76:2–10. doi: 10.1038/pr.2014.49
- Thursby E, Juge N. Introduction to the human gut microbiota. *Biochem J.* (2017) 474:1823–36. doi: 10.1042/BCJ20160510
- Conlon MA, Bird AR. The impact of diet and lifestyle on gut microbiota and human health. *Nutrients.* (2014) 7:17–44. doi: 10.3390/nu7010017
- Cockburn DW, Koropatkin NM. Polysaccharide degradation by the intestinal microbiota and its influence on human health and disease. *J Mol Biol.* (2016) 428:3230–52. doi: 10.1016/j.jmb.2016.06.021
- Zmora N, Suez J, Elinav E. You are what you eat: diet, health and the gut microbiota. *Nat Rev Gastroenterol Hepatol.* (2019) 16:35–56. doi: 10.1038/s41575-018-0061-2
- Gibson GR, Hutkins R, Sanders ME, Prescott SL, Reimer RA, Salminen SJ, et al. Expert consensus document: the international scientific association for probiotics and prebiotics (ISAPP) consensus statement on the definition and scope of prebiotics. *Nature Reviews Gastroenterology and Hepatology.* (2017) 14:491–502. doi: 10.1038/nrgastro.2017.75
- La Fata G, Rastall RA, Lacroix C, Harmsen HJM, Mohajeri MH, Weber P, et al. Recent development of prebiotic research-statement from an expert workshop. *Nutrients.* (2017) 9:1376. doi: 10.3390/nu9121376

8. Chen Z, Li S, Fu Y, Li C, Chen D, Chen H. Arabinoxylan structural characteristics, interaction with gut microbiota and potential health functions. *J Funct Foods*. (2019) 54:536–51. doi: 10.1016/j.jff.2019.02.007
9. Butardo VM Jr, Sreenivasulu N. Tailoring grain storage reserves for a healthier rice diet and its comparative status with other cereals. *Int Rev Cell Mol Biol*. (2016) 323:31–70. doi: 10.1016/b.sircmb.2015.12.003
10. Izydorczyk MS. Arabinoxylans. In: *Handbook of Hydrocolloids*. Cambridge: Woodhead Publishing Ltd (2009). p. 653–92. doi: 10.1533/9781845695873.653
11. Höije A, Sternemalm E, Heikkinen S, Tenkanen M, Gatenholm P. Material properties of films from enzymatically tailored arabinoxylans. *Biomacromolecules*. (2008) 9:2042–7. doi: 10.1021/bm800290m
12. Kivelä R, Henniges U, Sontag-Strohm T, Potthast A. Oxidation of oat β -glucan in aqueous solutions during processing. *Carbohydr Polym*. (2012) 87:589–97. doi: 10.1016/j.carbpol.2011.08.028
13. Bagdi A, Tömösközi S, Nyström L. Hydroxyl radical oxidation of feruloylated arabinoxylan. *Carbohydr Polym*. (2016) 152:263–70. doi: 10.1016/j.carbpol.2016.06.105
14. Bagdi A, Tömösközi S, Nyström L. Structural and functional characterization of oxidized feruloylated arabinoxylan from wheat. *Food Hydrocoll*. (2017) 63:219–25. doi: 10.1016/j.foodhyd.2016.08.045
15. Demuth T, Betschart J, Nyström L. Structural modifications to water-soluble wheat bran arabinoxylan through milling and extrusion. *Carbohydr Polym*. (2020) 240:116328. doi: 10.1016/j.carbpol.2020.116328
16. Roye C, Henrion M, Chanvrier H, De Roeck K, De Bondt Y, Liberloo I, et al. Extrusion-cooking modifies physicochemical and nutrition-related properties of wheat bran. *Foods*. (2020) 9:738. doi: 10.3390/foods9060738
17. Tuncil YE, Thakkar RD, Arioglu-Tuncil S, Hamaker BR, Lindemann SR. Subtle variations in dietary-fiber fine structure differentially influence the composition and metabolic function of gut microbiota. *mSphere*. (2020) 5:e00180–20. doi: 10.1128/mSphere.00180-20
18. Pastell H, Westermann P, Meyer AS, Tuomainen P, Tenkanen M. In vitro fermentation of arabinoxylan-derived carbohydrates by bifidobacteria and mixed fecal microbiota. *J Agric Food Chem*. (2009) 57:8598–606. doi: 10.1021/jf901397b
19. Feng G, Flanagan BM, Mikkelsen D, Williams BA, Yu W, Gilbert RG, et al. Mechanisms of utilisation of arabinoxylans by a porcine faecal inoculum: competition and co-operation. *Sci Rep*. (2018) 8:4546. doi: 10.1038/s41598-018-22818-4
20. Hughes SA, Shewry PR, Li L, Gibson GR, Sanz ML. In vitro fermentation by human fecal microflora of wheat arabinoxylans. *J Agric Food Chem*. (2007) 55:4589–95. doi: 10.1021/jf070293g
21. El Kaoutari A, Armougom F, Gordon JI, Raoult D, Henrissat B. The abundance and variety of carbohydrate-active enzymes in the human gut microbiota. *Nat Rev Microbiol*. (2013) 11:497–504. doi: 10.1038/nrmicro3050
22. Hald S, Schioldan AG, Moore ME, Dige A, Laerke HN, Agnholt J, et al. Effects of arabinoxylan and resistant starch on intestinal microbiota and short-chain fatty acids in subjects with metabolic syndrome: a randomised crossover study. *PLoS ONE*. (2016) 11:e0159223. doi: 10.1371/journal.pone.0159223
23. Damen B, Verspreet J, Pollet A, Broekaert WF, Delcour JA, Courtin CM. Prebiotic effects and intestinal fermentation of cereal arabinoxylans and arabinoxylan oligosaccharides in rats depend strongly on their structural properties and joint presence. *Mol Nutr Food Res*. (2011) 55:1862–74. doi: 10.1002/mnfr.201100377
24. Nguyen NK, Deehan EC, Zhang Z, Jin M, Baskota N, Perez-Munoz ME, et al. Gut microbiota modulation with long-chain corn bran arabinoxylan in adults with overweight and obesity is linked to an individualized temporal increase in fecal propionate. *Microbiome*. (2020) 8:118. doi: 10.1186/s40168-020-00887-w
25. Rumpagaporn P, Reuhs BL, Kaur A, Patterson JA, Keshavarzian A, Hamaker BR. Structural features of soluble cereal arabinoxylan fibers associated with a slow rate of in vitro fermentation by human fecal microbiota. *Carbohydr Polym*. (2015) 130:191–7. doi: 10.1016/j.carbpol.2015.04.041
26. De Paepe K, Verspreet J, Rezaei MN, Martinez SH, Meysman F, Van de Walle D, et al. Modification of wheat bran particle size and tissue composition affects colonisation and metabolism by human faecal microbiota. *Food Funct*. (2019) 10:379–96. doi: 10.1039/C8FO01272E
27. De Paepe K, Verspreet J, Courtin CM, Van de Wiele T. Wheat bran thermal treatment in a hot air oven does not affect the fermentation and colonisation process by human faecal microbiota. *J Funct Foods*. (2019) 60:103440. doi: 10.1016/j.jff.2019.103440
28. Roye C, Bulckaen K, De Bondt Y, Liberloo I, Van De Walle D, Dewettinck K, et al. Side-by-side comparison of composition and structural properties of wheat, rye, oat, and maize bran and their impact on in vitro fermentability. *Cereal Chem*. (2019) 97:20–33. doi: 10.1002/cche.10213
29. Deroover L, Tie Y, Verspreet J, Courtin CM, Verbeke K. Modifying wheat bran to improve its health benefits. *Crit Rev Food Sci Nutr*. (2020) 60:1104–22. doi: 10.1080/10408398.2018.1558394
30. Demuth T, Boulos S, Nyström L. Structural investigation of oxidized arabinoxylan oligosaccharides by negative ionization HILIC-qToF-MS. *Analyst*. (2020) 145:6691–704. doi: 10.1039/D0AN01110J
31. Hardy MR, Townsend RR, Lee YC. Monosaccharide Analysis of Glycoconjugates Chromatography with Pulsed Amperometric by Anion Exchange Detection. *Anal Biochem*. (1988) 170:54–62. doi: 10.1016/0003-2697(88)90089-9
32. Rohrer JS, Cooper GA, Townsend RR. Identification, quantification and characterization of glycopeptides in reversed-phase HPLC separations of glycoprotein proteolytic digests. *Anal Biochem*. (1993) 212:7–16. doi: 10.1006/abio.1993.1283
33. Werner RA, Bruch BA, Brand WA. An interface for high precision $\delta_{13}\text{C}$ and $\delta_{15}\text{N}$ analysis with an extended dynamic range. *Rapid Commun Mass Spectrom*. (1999) 13:1237–41. doi: 10.1002/(SICI)1097-0231(19990715)13:13<1237::AID-RCM633>3.0.CO;2-C
34. Brooks PD, Geilmann H, Werner RA, Brand WA. Improved precision of coupled $\delta_{13}\text{C}$ and $\delta_{15}\text{N}$ measurements from single samples using an elemental analyzer/isotope ratio mass spectrometer combination with a post-column six-port valve and selective CO_2 trapping; improved halide robustness of the combustion reactor using CeO_2 . *Rapid Commun Mass Spectrom*. (2003) 17:1924–6. doi: 10.1002/rcm.1134
35. Sosulski FW, Imafidon GI. Amino acid composition and nitrogen-to-protein conversion factors for animal and plant foods. *J Agric Food Chem*. (1990) 38:1351–6. doi: 10.1021/jf00096a011
36. Lupo C, Boulos S, Nyström L. Influence of partial acid hydrolysis on size, dispersity, monosaccharide composition, and conformation of linearly-branched water-soluble polysaccharides. *Molecules*. (2020) 25:2982. doi: 10.3390/molecules25132982
37. Berner AZ, Fuentes S, Dostal A, Payne AN, Gutierrez PV, Chassard C, et al. Novel polyfermentor intestinal model (PolyFermS) for controlled ecological studies: validation and effect of pH. *PLoS ONE*. (2013) 8:e77772. doi: 10.1371/journal.pone.0077772
38. Poeker SA, Geirnaert A, Berchtold L, Greppi A, Krych L, Steinert RE, et al. Understanding the prebiotic potential of different dietary fibers using an in vitro continuous adult fermentation model (PolyFermS). *Sci Rep*. (2018) 8:4318. doi: 10.1038/s41598-018-22438-y
39. Macfarlane GT, Macfarlane S, Gibson GR. Validation of a three-stage compound continuous culture system for investigating the effect of retention time on the ecology and metabolism of bacteria in the human colon. *Microb Ecol*. (1998) 35:180–7. doi: 10.1007/s002489900072
40. Duncan SH, Hold GL, Harmsen HJ, Stewart CS, Flint HJ. Growth requirements and fermentation products of *Fusobacterium prausnitzii*, and a proposal to reclassify it as *Faecalibacterium prausnitzii* gen. nov, comb nov. *Int J Syst Evol Microbiol*. (2002) 52:2141–6. doi: 10.1099/00207713-52-6-2141
41. Michel C, Kravtchenko TP, David A, Gueneau S, Kozłowski F, Cherbut C. In vitro prebiotic effects of Acacia gums onto the human intestinal microbiota depends on both botanical origin and environmental pH. *Anaerobe*. (1998) 4:257–66. doi: 10.1006/anae.1998.0178
42. Pritchard SE, Marciani L, Garsed KC, Hoad CL, Thongborisute W, Roberts E, et al. Fasting and postprandial volumes of the undisturbed colon: normal values and changes in diarrhea-predominant irritable bowel syndrome measured using serial MRI. *Neurogastroenterol Motility*. (2014) 26:124–30. doi: 10.1111/nmo.12243
43. Micha R, Khatibzadeh S, Shi P, Andrews KG, Engell RE, Mozaffarian D. Global, regional and national consumption of major food groups in 1990 and 2010: a systematic analysis including 266 country-specific nutrition surveys worldwide. *BMJ Open*. (2015) 5:e008705. doi: 10.1136/bmjopen-2015-008705

44. Rinttila T, Kassinen A, Malinen E, Krogius L, Palva A. Development of an extensive set of 16S rDNA-targeted primers for quantification of pathogenic and indigenous bacteria in faecal samples by real-time PCR. *J Appl Microbiol.* (2004) 97:1166–77. doi: 10.1111/j.1365-2672.2004.02409.x
45. Fierer N, Jackson JA, Vilgalys R, Jackson RB. Assessment of soil microbial community structure by use of taxon-specific quantitative PCR assays. *Appl Environ Microbiol.* (2005) 71:4117–20. doi: 10.1128/AEM.71.7.4117-4120.2005
46. Furet JP, Firmesse O, Gourmelon M, Bridonneau C, Tap J, Mondot S, et al. Comparative assessment of human and farm animal faecal microbiota using real-time quantitative PCR. *FEMS Microbiol Ecol.* (2009) 68:351–62. doi: 10.1111/j.1574-6941.2009.00671.x
47. Stoddard SE, Smith BA-OX, Hein R, Roller BA-O, Schmidt TM. rrnDB: improved tools for interpreting rRNA gene abundance in bacteria and archaea and a new foundation for future development. *Nucleic Acids Res.* (2015) 43:D593–8 doi: 10.1093/nar/gku1201
48. Callahan BJ, McMurdie PJ, Rosen MJ, Han AW, Johnson AJ, Holmes SP. DADA2: High-resolution sample inference from Illumina amplicon data. *Nat Methods.* (2016) 13:581–3. doi: 10.1038/nmeth.3869
49. Glockner FO, Yilmaz P, Quast C, Gerken J, Beccati A, Ciuprina A, et al. 25 years of serving the community with ribosomal RNA gene reference databases and tools. *J Biotechnol.* (2017) 261:169–76. doi: 10.1016/j.jbiotec.2017.06.1198
50. Bolyen E, Rideout JR, Dillon MR, Bokulich NA, Abnet CC, Al-Ghalith GA, et al. Reproducible, interactive, scalable and extensible microbiome data science using QIIME 2. *Nat Biotechnol.* (2019) 37:852–7. doi: 10.1038/s41587-019-0209-9
51. McMurdie PJ, Holmes S. phyloseq: an R Package for reproducible interactive analysis and graphics of microbiome census data. *PLoS ONE.* (2013) 8:e61217. doi: 10.1371/journal.pone.0061217
52. Love MI, Huber W, Anders S. Moderated estimation of fold change and dispersion for RNA-seq data with DESeq2. *Genome Biol.* (2014) 15:550. doi: 10.1186/s13059-014-0550-8
53. Team RC. *R: A Language and Environment for Statistical Computing.* Vienna: R Foundation for Statistical Computing (2014).
54. Ralet MC, Thibault JF, Della Valle JG. Influence of extrusion-cooking on the physico-chemical properties of wheat bran. *J Cereal Sci.* (1990) 11:249–59. doi: 10.1016/S0733-5210(09)80169-0
55. Gollner EM, Blaschek W, Classen B. Structural investigations on arabinogalactan-protein from wheat, isolated with Yariv reagent. *J Agric Food Chem.* (2010) 58:3621–6. doi: 10.1021/jf903843f
56. Diether NE, Willing BP. Microbial fermentation of dietary protein: an important factor in diet-microbe-host interaction. *Microorganisms.* (2019) 7:19. doi: 10.3390/microorganisms7010019
57. Van den Abbeele P, Gerard P, Rabot S, Bruneau A, El Aidy S, Derrien M, et al. Arabinoxylans and inulin differentially modulate the mucosal and luminal gut microbiota and mucin-degradation in humanized rats. *Environ Microbiol.* (2011) 13:2667–80. doi: 10.1111/j.1462-2920.2011.02533.x
58. Belobrajdic DP, Bird AR, Conlon MA, Williams BA, Kang S, McSweeney CS, et al. An arabinoxylan-rich fraction from wheat enhances caecal fermentation and protects colonocyte DNA against diet-induced damage in pigs. *Br J Nutr.* (2012) 107:1274–82. doi: 10.1017/S0007114511004338
59. Nordlund E, Aura AM, Mattila I, Kössö T, Rouau X, Poutanen K. Formation of phenolic microbial metabolites and short-chain fatty acids from rye, wheat, and oat bran and their fractions in the metabolic in vitro colon model. *J Agric Food Chem.* (2019) 60:8134–45. doi: 10.1021/jf3008037
60. Rose DJ, Patterson JA, Hamaker BR. Structural differences among alkali-soluble arabinoxylans from maize (*Zea mays*), rice (*Oryza sativa*), and wheat (*Triticum aestivum*) brans influence human fecal fermentation profiles. *J Agric Food Chem.* (2010) 58:493–9. doi: 10.1021/jf9020416
61. Van Craeyveld V, Swennen K, Dornez E, Van de Wiele T, Marzorati M, Verstraete W, et al. Structurally different wheat-derived arabinoxyloligosaccharides have different prebiotic and fermentation properties in rats. *J Nutr.* (2008) 138:2348–55. doi: 10.3945/jn.108.094367
62. Snelders J, Olaerts H, Dornez E, Van de Wiele T, Aura A-M, Vanhaecke L, et al. Structural features and feruloylation modulate the fermentability and evolution of antioxidant properties of arabinoxylanoligosaccharides during *in vitro* fermentation by human gut derived microbiota. *J Funct Foods.* (2014) 10:1–12. doi: 10.1016/j.jff.2014.05.011
63. Kjolbaek L, Benitez-Paez A, Gomez Del Pulgar EM, Brahe LK, Liebisch G, Matsysik S, et al. Arabinoxylan oligosaccharides and polyunsaturated fatty acid effects on gut microbiota and metabolic markers in overweight individuals with signs of metabolic syndrome: a randomized cross-over trial. *Clin Nutr.* (2020) 39:67–79. doi: 10.1016/j.clnu.2019.01.012
64. Riviere A, Selak M, Lantin D, Leroy F, De Vuyst L. Bifidobacteria and butyrate-producing colon bacteria: importance and strategies for their stimulation in the human gut. *Front Microbiol.* (2016) 7:979. doi: 10.3389/fmicb.2016.00979
65. Chung WSE, Walker AW, Bosscher D, Garcia-Campayo V, Wagner J, Parkhill J, et al. Relative abundance of the *Prevotella* genus within the human gut microbiota of elderly volunteers determines the inter-individual responses to dietary supplementation with wheat bran arabinoxylan-oligosaccharides. *BMC Microbiol.* (2020) 20:283. doi: 10.1186/s12866-020-01968-4
66. Louis P, Flint HJ. Formation of propionate and butyrate by the human colonic microbiota. *Environ Microbiol.* (2017) 19:29–41. doi: 10.1111/1462-2920.13589
67. Lopez-Siles M, Duncan SH, Garcia-Gil LJ, Martinez-Medina M. Faecalibacterium prausnitzii: from microbiology to diagnostics and prognostics. *ISME J.* (2017) 11:841–52. doi: 10.1038/ismej.2016.176
68. Borges A, Ferreira C, Saavedra MJ, Saavedra MJ, Simões M. Antibacterial activity and mode of action of ferulic and gallic acids against pathogenic bacteria. *Microb Drug Resist.* (2013) 19:256–65. doi: 10.1089/mdr.2012.0244
69. Hopkins MJ, Englyst HN, Macfarlane S, Furrie E, Macfarlane GT, McBain AJ. Degradation of cross-linked and non-cross-linked arabinoxylans by the intestinal microbiota in children. *Appl Environ Microbiol.* (2003) 69:6354–60. doi: 10.1128/AEM.69.11.6354-6360.2003
70. Grant LJ, Mikkelsen D, Phan ADT, Kang S, Ouwerkerk D, Klieve AV, et al. Purified plant cell walls with adsorbed polyphenols alter porcine faecal bacterial communities during *in vitro* fermentation. *Food Funct.* (2020) 11:834–45. doi: 10.1039/C9FO02428J
71. Zhang X, Chen T, Lim J, Xie J, Zhang B, Yao T, et al. Fabrication of a soluble crosslinked corn bran arabinoxylan matrix supports a shift to butyrogenic gut bacteria. *Food and Function.* (2019) 10:4497–504. doi: 10.1039/C8FO02575D
72. De Paepel KA-O, Kerckhof FM, Verspreet J, Courtin CM, Van de Wiele T. Inter-individual differences determine the outcome of wheat bran colonization by the human gut microbiome. *Environ Microbiol.* (2017) 19:3251–67. doi: 10.1111/1462-2920.13819
73. Cantu-Jungles TM, Hamaker BR. New View on Dietary Fiber Selection for Predictable Shifts in Gut Microbiota. *MBio.* (2020) 11:e02179–e02119. doi: 10.1128/mBio.02179-19

Conflict of Interest: The authors declare that the research was conducted in the absence of any commercial or financial relationships that could be construed as a potential conflict of interest.

Publisher's Note: All claims expressed in this article are solely those of the authors and do not necessarily represent those of their affiliated organizations, or those of the publisher, the editors and the reviewers. Any product that may be evaluated in this article, or claim that may be made by its manufacturer, is not guaranteed or endorsed by the publisher.

Copyright © 2021 Demuth, Edwards, Bircher, Lacroix, Nyström and Geirnaert. This is an open-access article distributed under the terms of the Creative Commons Attribution License (CC BY). The use, distribution or reproduction in other forums is permitted, provided the original author(s) and the copyright owner(s) are credited and that the original publication in this journal is cited, in accordance with accepted academic practice. No use, distribution or reproduction is permitted which does not comply with these terms.